中國機械工程學刊第四十一卷第五期第 639~646 頁(民國一百零九年)
Journal of the Chinese Society of Mechanical Engineers, Vol.41, No.5, pp 639~646 (2020)

Friction Stir Spot Welding of PLA-PEKK-HAp-CS Based 3D Printed Scaffolds for Minor Repair

Rupinder Singh[,**], Jaskarn Singh[*], Gurchetan Singh[*] and Ranvijay Kumar[*,***]

Keywords：Friction stir spot welding, Consumable tool, PLA-PEKK-Hap-CS, Fused deposition modelling

ABSTRACT

The 3D printed thermoplastic composites of polylactic acid (PLA) are commercially used as biomedical scaffolds/ implants in tissue engineering applications. But hitherto limited studies have been reported on use of joining techniques in repair of 3D printed biomedical scaffolds. In this study, functional prototypes of PLA reinforced with poly ether ketone ketone (PEKK)- hydroxyapatite (HAp)- chitosan (CS) were 3D printed as scaffolds with fused deposition modelling (FDM), followed by their joining with friction stir spot wielding (FSSW) as a novel route. The scaffold joint were investigated for mechanical and morphological properties for possible online repair of minor surface defects. The outcomes of this case study suggest that 1000rpm rotational speed, 2mm consumable pin depth and 20 sec stirring time are best settings for strength and surface hardness of the 3D printed scaffold joints.

INTRODUCTION

Due to the low cost of FDM based 3D printer in generating complex shapes with a simple setup, this process gets significant attention in today's commercial manufacturing field. In this process monofilament is extruded from heated nozzle head, which is guided by servo motors in order to move in 3D planes (Rodríguez et al., 2001). As compared to other manufacturing processes this process gives end product in a single step.

Paper Receivedr September, 2019. Revised December, 2019. Accepted February, 2020. Author for Correspondence: Rupinder Singh

[*] *Department of Production Engineering, Guru Nanak Dev Engineering College, Ludhiana (India)*

[**] *Department of Mechanical Engineering, NITTTR, Chandigarh (India)*

[***] *University Center for Research and Development, Chandigarh University, Mohali (India)*

Also due to printing of parts in layers and fine control of operating parameters (like: infill density, temperature control etc.) it is easy to control the end product mechanical properties (Adam and Zimmer, 2015). The printing nozzle is numerically control by programmed software that ultimately increases the manufacturing accuracy. During printing the thermal shrinkage of printed part play key role in maintaining desirable shape as well as properties due to variation in rate of heat transfer at different datum (Ahn et al., 2002; Benjamin et al., 2018). The ability to make complex design and assemblies, less floor space for installment, fast manufacturing and more variables are major benefits of this process over other traditional manufacturing process. In its starting stages this process is used in making prototype of tools and machines, 3D map of house and city, bridge and dam modeling etc. (Croccolo et al., 2013). Currently this printing field is limited for the printing of polymers which are not as stronger as that of metals so 3D printed parts are not used in any major load carrying applications. The main building variables are: nozzle temperature, bed temperature, builds direction, filament cross section, raster angle, layer thickness and air gap (Dizon et al., 2018). Before making the final product it is necessary to analyze the stress on the each section of the part. Because by varying operating parameter different mechanical properties could be achieved at different section. Although it is observed that mechanical behavior of printed parts is closer to injected molded parts. Durgunand Ertan (2014) optimized the process parameter of FDM process in order to get best mechanical properties. It has been concluded that build orientation is more considerable factor than raster angle to get surface finish and mechanical properties. Close connection is observed in mechanical properties and surface roughness (Es-Said et al., 2000). During printing of ABS polymer it has observed that due to phase conversion (semi liquid to solid) shrinkage may result into deviation of actual dimension of the printed part from modeled one. Sometimes pores are generated and weak bonding also takes place between the layers which result in anisotropy behavior of the printed part (Fatimatuzahraa et al., 2011). Porosity is also a considerable factor to investigate the mechanical behavior of the printed part that is influenced by the filament cross section and air gap. The flow ability of the polymer is an important property that significantly helps to fill the voids or air gap inside the printed part. The interface bonding between the layers significantly affect the structural integrity and affect the shear behavior of the printed part (Baich et al., 2015). Mechanical properties are greatly influenced by lattice orientation of printed structure. Among the different structure design honeycomb design shows best mechanical properties. More than two times increase in mechanical properties can be gained by honeycomb structure then double dense structure design. Lee et al. (11) determined the strain energy storing capability of the ABS printed specimen by means of ball thrown test. The air gap in the printed job gives maximum contribution at the thrown angle of 10°. At thrown angle of 15^o and 20^o layer thickness gives maximum contribution in storing strain energy (Onwubolu and Rayegani, 2014). It has been reported that smaller layer thickness, negative air gap and minimum raster width significantly improve the tensile strength of the printed job of ABS material. Printed job orientation also play considerable role in the tensile strength of the specimen. If the printing direction is parallel to the loading direction then maximum strength is observed (Rankouhi et al., 2016). Rankouhi et al. investigated the failure of ABS printed samples. It was seen that layer thickness of 0.2mm is stronger in tensile testing then the 0.4mm layer thickness. It was concluded from the microscopic examination that minimum voids contribute to the best mechanical properties (Rankouhi et al., 2018). Molecule alignment is greatly influenced by the raster orientation which significantly affects the mechanical properties of the printed sample. The ambient condition of the printed sample space affects the solidification rate of the extruded filament which ultimately affects the interlayer bonding (Sood et al., 2010).

Friction stir welding (FSW) drastically seek the attention of today researcher due to its less thermal effect on joint. The rotating pin in rotor generate heat due to friction between rubbing surface and mechanical mixing also ensure in good bonding of the joint (Vijendra and Sharma, 2015). The operating parameter of FSW such as rotational speed, indentation depth, longitudinal speed or feed, axial load and tilt angle significantly affect the mechanical properties of the joint. As per reported literature blow holes are observed at low rotational speed due to incomplete bonding between the interfacing sides (Jaiganesh et al., 2014). The tensile strength of the friction welded joint is greatly influenced by the rotational as well as longitudinal speed. It was concluded from visual inspection that more defect take place at the retarding side of the sample joint (Eslami et al., 2015; Węglowska and Pietras. 2012). Some researchers have reported friction welding of dissimilar polymer materials with metal powder reinforcement for engineering applications (Singh et al., 2016; Kumar et al., 2018a; Kumar et al., 2018b). Also weldability of thermoplastic composites in FSW has been investigated for acrylonitrile butadiene styrene (ABS) and poly amide (PA) sheets with semi consumable tool (Kumar et al., 2018c; Kumar et al., 2019). Singh et al. has reported the PLA-PEKK-HAp-CS composite scaffold joining with FSSW by using compression moulded samples. In this study ultimate tensile strength of 6.57MPa was observed (Singh et al., 2019a).

Tian et al. investigated the effect of carbon fiber on PLA parts by means of 3D printing. The flexural strength and modulus of the specimen are found to be 335MPa and 30GPa respectively in 27% reinforcement level of carbon fibers (Tian et al., 2016).Some researchers have prepared scaffolds of PLA based composite material with 3D printing, by adding small amount (5%) of polyethylene glycol with high resolution PLA (Serra et al., 2016). Senatov et al. analyzed the mechanical behavior of porous scaffolds of PLA polymer matrix prepared with 3D printing. In this study composite with 15% HAp and 85% PLA has been recommended for small bone implants (Senatov et al., 2016). Some studies have reported tensile, compressive and morphological properties of 3D printed functional prototypes of PLA-PEKK-HAp-CS, which was influenced by infill speed and infill density while 3D printing. Also some work has been reported on development of feed stock filament of PLA matrix and its joining capabilities especially in biomedical applications (Singh et al., 2019b; Ranjan et al., 2018; Ranjan et al., 2019).

The literature review reveals that in past three decades many studies were focused on preparations and development of PLA and other biocompatible thermoplastic composites for potential use in biomedical applications (especially with FDM printed functional prototypes). But hitherto little has been reported on use of joining techniques for minor repair of 3D printed biomedical scaffolds. It is expected that while FSSW of FDM printed parts, the grain orientation of reinforcements and PLA matrix as binder may lead to uniform grain distribution/ dispersion resulting into better adoption of grain boundaries along the contour of joint surface (which may result into improved mechanical properties). In this study, the PLA matrix reinforced with PEKK-HAp-CS based functional prototypes were 3D printed as scaffolds followed by their joining with FSSW with consumable tool as a novel method. This study is extension of work reported by Singh et al. 2019a; Ranjan et al., 2018; Ranjan et al., 2019, in which PLA-PEKK-HAp-CS composite based feed stock filament was prepared and compression moulded samples were processed with FSSW.

EXPERIMENTATION

The PLA thermoplastic was reinforced with PEKK, HAp and CS powder in this study. The filaments of different compositions/ proportions were mechanically tested on universal testing machine (UTM). To get best parts from the 3D printing, different parameter (like: infill density/ratio, infill speed and no. of perimeters) were selected and printed specimens were tested on UTM. The levels of input parameters were selected based upon pilot experimentation. Table 1 shows the data of tensile strength of FDM printed functional prototype by following Taguchi L9 based orthogonal array (OA).

Table 1: 3D printing parameters and observed peak strength values

S. No.	Infill speed (mm/s)	No of perimeters	Infill ratio (%)	Peak strength in tension (MPa)
1.	50	3	60	24.48±0.31
2.	60	4	60	29.75±0.60
3.	70	5	60	19.40±0.22
4.	50	4	80	35.16±0.32
5.	60	5	80	35.49±0.53
6.	70	3	80	30.20±0.23
7.	50	5	100	42.29±0.31
8.	60	3	100	38.51±0.43
9.	70	4	100	37.08±0.35

It should be noted that three repetitions were made and average values for peak strength has been mentioned.

As observed from the Table 1, sample no.7 shows the best mechanical strength in tensile test. The printing parameter of this sample was 100% infill ratio, 50mm/sec infill speed and 5number of perimeters. In order to further proceed towards the optimization of joint strength properties, the printing parameter of sample 7 (Table 1) were selected.

For the optimization of FSSW the parameters namely: rotational speed, plunging depth/ consumable pin depth and welding/ stirring time were selected based upon pilot experimentation. Fig. 1 shows 3D printed specimens prepared at 100% infill ratio, 50mm/s infill speed and 5number of perimeters.

Fig. 1: 3D printed specimen

During pilot experimentation it has been observed that in order to make proper bond between the 3D printed samples minimum 800 rpm rotational speed was required. The printed part thickness was 4mm, so the plunging depth of 2-3mm was selected. It was also observed during pilot experimentation that minimum 15s time is required for sufficient heating to make proper bond. Table 2 shows the different operating parameter arranged as per Taguchi L9 O.A for investigations of FSSW joint properties.

Table 2: Welding parameters as per Taguchi L9 O.A

S. No.	A Rotational speed (rpm)	B Consumable pin depth (mm)	C Stirring time (s)
1.	800	2	15
2.	800	2.5	20
3.	800	3	25
4.	1000	2	20
5.	1000	2.5	25
6.	1000	3	15
7.	1200	2	25
8.	1200	2.5	15
9.	1200	3	20

Note: Three repetitions were made to reduce the experimental errors.

Pins to be used as filler (Fig. 2) were also printed on FDM as per settings suggested in Table 1 (S. No. 7). The diameter of the cylindrical pin was 4mm.

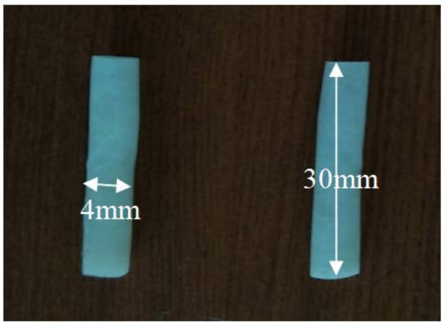

Fig. 2: FDM printed consumable pins for FSSW

The pins ware fitted in the tool holder and set at desire depth. Fig.3 shows the setup for FSSW. The printed sample was set on the machine bed by means of holding plates with the help of locators. The pin was rigidly mounted inside the tool holder with the help of hexagonal bolt as shown in the Fig. 3.

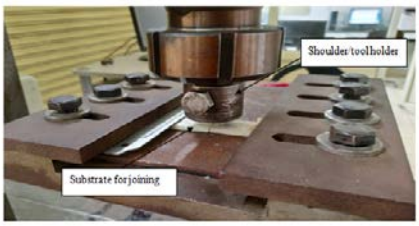

Fig. 3: Welding setup for FSSW on vertical milling machine

Total nine joints were prepared with three repetitions as per Table 2. Fig. 4 shows the joint prepared by FSSW process. As observed from Fig. 4 uniformly stirred (thermo-mechanical affected) zone was observed with FSSW. The pin at welded zone was removed by mechanical cutting and grinding. The excess flash produced due to polymer flow out of joint was also removed by grinding. After this Shore

D hardness was measured on the welding zone of the samples. The three readings were taken from surface and average of three was taken as final hardness of that sample. In order to understand the effect of processing parameters on mechanical properties of the joints, the tensile test was performed on universal tensile testing machine (UTM) at 50mm/min elongation rate. Fig. 5 shows the setup of sample for the tensile test on UTM (at 50mm/min speed).

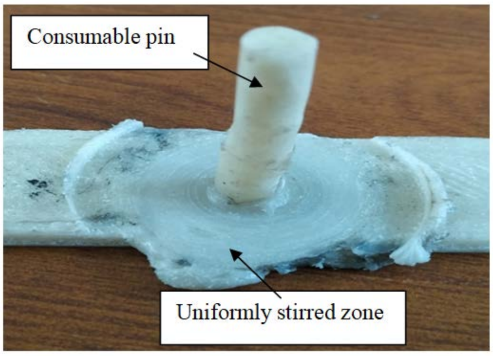

Fig. 4 FSSW joint

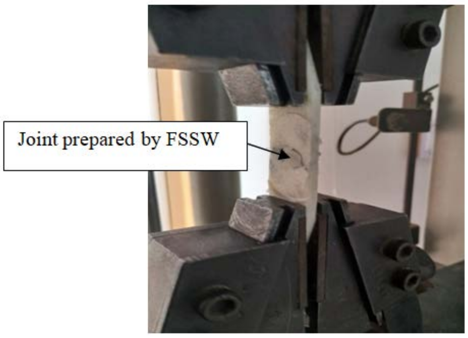

Fig. 5: UTM setup

In this study standard dimensions of dumbbell shape for tensile testing as per ASTM D 638 were not used, but for commercial applications of FSSW based joining standard samples needs to be compared. Since this work is primarily focused on development of novel route for joining of PLA matrix based scaffolds/ implants hardly one will encounter standard shape/ dimensions as per ASTM D 638. However to control the error three repetitions were made for each experimental observation. Table 3 shows the observations for Shore D hardness and peak strength of each sample as per Table 2.

Table 3: Observed hardness and peak strength of samples

S. No.	Shore D hardness of the welding zone	Peak strength (MPa)
1.	53±1.0	1.9±0.1
2.	64±2.0	12.5±0.3
3.	59±0.5	2.6±0.1
4.	72±1.0	22.0±0.9
5.	66±2.0	8.9±0.5
6.	60±0.5	6.5±0.2
7.	68±1.0	5.9±0.1
8.	52±0.5	1.4±0.1
9.	71±1.0	7.5±0.3

It has been observed from the Table 3, sample at S.No.4 shows maximum hardness, which was prepared at welding time of 20s and depth of 2mm and at the rotational speed of 1000rpm. It should be noted that the stirring time plays crucial role in surface hardness. Increasing the welding/ stirring time increases the flow ability of polymer composite hence more material may get deposited in welding zone. Higher speed of rotation increases the rate of heat generation as well as thrust force which increase the flow ability of polymer. This removes maximum material as a flash and lower down the surface hardness of the weld zone. It has been observed during testing that the failure took place near the faces to be joined and not on the joint surface in all welding samples. As observed from the Table 3, maximum peak strength was obtained for sample at S.No.4 (22±0.9 MPa). Overall the effect of single/ combined factors (input parameters) of FSSW may be responsible for variation in hardness/ tensile properties. To understand/ ascertain the effect of each input parameter further statistical analysis was conducted.

RESULTS AND DISCUSSION

Based upon Table 3, Table 4 shows signal to noise (SN) ratio analysis for peak strength and Shore D hardness for larger the better type case.

Table 4: SN ratio of peak strength in tensile test

S. No.	Peak strength in tensile test (×10MPa)	SN ratio (dB)	Shore D Hardness	SN ratio (dB)
1	0.19	-14.42	53	34.48
2	1.25	1.93	64	36.12
3	0.26	-11.70	59	35.41
4	2.20	6.84	72	37.14
5	0.89	-1.01	66	36.39
6	0.65	-3.74	60	35.56
7	0.59	-4.58	68	36.65
8	0.14	-17.07	52	34.32
9	0.75	-2.49	71	37.02

Based upon Table 4, Fig. 6 shows the main effect plot for peak strength. As observed from Fig. 6, 1000rpm rotational speed, 2mm pin depth and 20 s welding time are the best settings for mechanical strength of the joints. The increase in SN ratio from 800 to 1000rpm is but obvious as high rpm will result into more heat generation leading to better flow of material. Further decrease in SN ratio, with increase in rpm from 1000 to 1200 may be because of the fact that high rpm results into more flash generation and thinning of the joint section. Similar trend has been observed in case of stirring time. On the other hand, axial depth along the thickness directly decrease the cross-section area of joint which decrease the strength of joint, the same has been observed in Fig. 6.

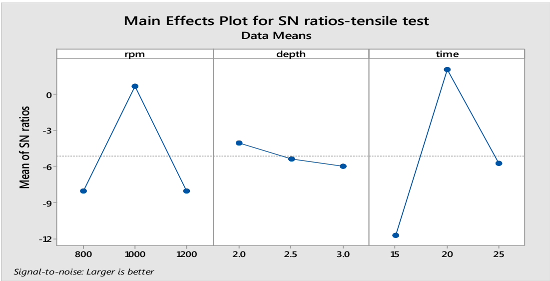

Fig. 6 Influence of input-variables (on peak strength in tensile test)

Based upon Table 4, Table 5 shows the analysis of variance (ANOVA) for peak strength.

Table 5: ANOVA for peak strength

Input	DF	SS	Adj. SS	Adj. MS	F	P	%C
A	2	153.33	153.33	76.66	3.53	0.22	31.17%
B	2	5.84	5.84	2.92	0.13	0.88	1.19%
C	2	289.24	289.24	144.62	6.66	0.13	58.81%
Residual error	2	43.43	43.43	21.71			8.83%
Total	8	491.85					

Note: DF: Degree of freedom, SS: Sum of Squares, Adj. SS: Adjacent sum of squares, Adj. MS: Adjacent mean of squares, F: Fisher's value, P: Probability, %C: Percentage contribution

As observed from Table 5, welding/ stirring time is a major parameter which decides the mechanical strength of the joint. Further based upon Table 5, Table 6 shows ranking of input parameters for peak strength.

Table 6: Ranking table for peak strength (larger is better)

Level	A	B	C
1	-8.06	-4.05	-11.74
2	0.69	-5.38	2.09
3	-8.05	-5.98	-5.76
Delta	8.76	1.92	13.84
Rank	2	3	1

Empirical model for prediction of peak strength: For prediction of optimum value of peak strength following equation has been used:

$a_{opt} = b + (b_{A2} - b) + (b_{B1} - b) + (b_{C2} - b)$

a_{opt} = optimum SN ratio value (for peak strength in tensile test)

b = overall average of SN data

b_{A2} = average of SN data for rotation speed at level 2

b_{B1} = average of SN data for pin depth at level 1

b_{C2} = average of SN data for stirring time at level 2

$c_{opt}2 = (10)\ a_{opt}/10$ (to be used in case of properties, where larger is better)

b= -5.13 dB

b_{A2} = 0.69

b_{B1} = -4.05

b_{C2} = 2.09

a_{opt} = -5.13 + (0.69+5.13) + (-4.05+5.13) + (2.09+5.13)

a_{opt} = 8.99 dB

$c_{opt}2 = (10)\ a_{opt}/10$

$c_{opt}2 = (10)\ 8.99/10$

c_{opt} = 2.78

Predicted value of peak strength at optimum setting = 2.78×10MPa, where as actual observed value is 2.2×10MPa (see Table 4, Exp. No. 4). This variation may be explained based upon the fact that PLA is semi crystalline material and reinforcement of PEKK, HAp and CS may have contributed as heat sink, and residual error of 8.86% was observed (see Table 6) and no input parameter was found significant at 95% confidence level. In order to address this issue two factor interaction (2FI) in historical data approach (under response surface methodology) has been applied (using commercial Design Expert software). Table 7 shows ANOVA based upon 2FI for peak strength.

Table 7: ANOVA based upon response surface 2FI model for peak strength (using historical data approach)

Input	SS	DF	MS	F	P	
Model	469.94	6	78.32	3.80	0.0267	Significant
A	218.25	1	218.25	10.60	0.0077	Significant
B	297.00	1	297.00	14.42	0.0030	Significant
C	237.86	1	237.86	11.55	0.0059	Significant
AB	278.68	1	278.68	13.53	0.0036	Significant
AC	256.90	1	256.90	12.47	0.0047	Significant
BC	346.07	1	346.07	16.80	0.0018	Significant

As observed from Table 7, the 2FI model is significant with all input parameters. Based upon Table 7, final Equation in terms of actual factors is given as:

Peak strength = -129.54-0.095 ×(rotational speed)-26.9 × (consumable pin depth)+24.01 × (stirring time)+0.109 × (rotational speed) × (consumable pin depth)-0.01 × (rotational speed) × (stirring time) -4.87 × (consumable pin depth) × (stirring time) ----------------------------(1)

Further based upon observation in Table 3, Fig. 7 shows main effect plot for SN ratio of shore D hardness.

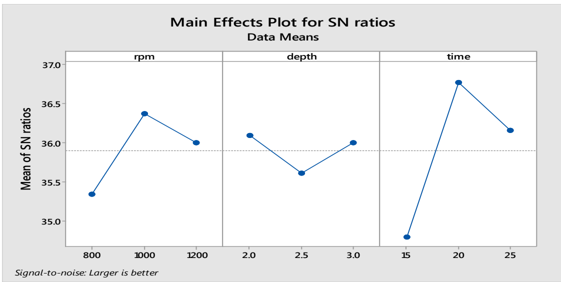

Fig. 7: SN plot for Shore D hardness

As observed from Fig. 7, the best setting of input parameters is similar to Fig. 6. Further, based upon Table 3, Table 8 and 9 respectively shows ANOVA responses and ranking of input parameters for Shore D hardness.

Table 8: ANOVA for shore D hardness

Input	DF	SS	Adj. SS	Adj. MS	F	P	%C
A	2	1.61	1.61	0.80	4.36	0.18	18.98%
B	2	0.39	0.39	0.19	1.06	0.48	4.62%
C	2	6.13	6.13	3.06	16.55	0.05	72.04%
Residual error	2	0.37	0.37	0.18			4.35%
Total	8	8.51					

Table 9: Ranking table for Shore D hardness (larger is better)

Level	Rotational speed	Consumable pin depth	Stirring time
1	35.34	36.09	34.79
2	36.37	35.61	36.77
3	36.00	36.00	36.15
Delta	1.02	0.48	1.98
Rank	2	3	1

Empirical model for prediction of Shore D hardness: For prediction of optimum value of Shore D hardness following equation has been used:

$a_{opt} = b + (b_{A2} - b) + (b_{B1} - b) + (b_{C2} - b)$

a_{opt} = optimum SN ratio value (for hardness in shore D test)

b = overall average of SN data

b_{A2} = average of SN data for rotation speed at level 2

b_{B1} = average of SN data for pin depth at level 1

b_{C2} = average of SN data for stirring time at level 2

$c_{opt}2 = (10)\ a_{opt}/10$ (to be used in case of properties, where larger is better)

b= 35.90 dB

b_{A2} = 36.37

b_{B1} = 36.09

b_{C2} = 36.77

a_{opt} = 35.90 + (36.37 – 35.90) + (36.09 – 35.90) + (36.77 – 35.90)

a_{opt} = 37.43 dB

$copt2 = (10)^{a_{opt}/10}$

$c_{opt}2 = (10)\ 37.43/10$

c_{opt} = 74.39

The predicted hardness = 74.39 Shore D and observed value is 72 (Table 3, Exp. No. 4).

As observed from Table 8 no parameter is significant at 95% confidence level. In order to address this issue two factor interaction (2FI) in historical data approach (under response surface methodology) has been applied (using commercial Design Expert software). Table 10 shows ANOVA based upon 2FI.

Table 10: ANOVA based upon response surface 2FI model for Shore D hardness (using historical data approach)

Input	SS	DF	MS	F	P	
Model	629.33	6	104.89	5.20	0.0091	Significant
A	18.11	1	18.11	0.90	0.3636	Not-Significant
B	30.96	1	30.96	1.54	0.2410	Not-Significant
C	462.01	1	462.01	22.92	0.0006	Significant
AB	207.43	1	207.43	10.29	0.0083	Significant
AC	34.71	1	34.71	1.72	0.2162	Not-Significant
BC	177.19	1	177.19	8.79	0.0129	Significant

As observed from Table 10, the 2FI model is significant for Shore D hardness. Based upon Table 10, final equation in terms of actual factors is given as:

Shore D hardness = +30.97×(rotational speed) -0.16× (rotational speed) -29.43× (consumable pin depth) +14.45 × (stirring time)+ +0.094× (rotational speed) × (consumable pin depth)-3.85× 10-3(rotational speed) × (stirring time)-3.48× (consumable pin depth)× (stirring time)---- (2)

Surface porosity

As observed from the Table 3, sample at S.No. 4 show maximum peak strength and surface hardness and sample at S.No. 8 show poor properties. For better understanding porosity level of these samples were calculated as per ASTM E2015-04(2014) at ×100 magnification (Fig. 8a). These optical photomicrographs were further processed to get 3D rendered images (Fig. 8b) and surface roughness (Ra) profile (Fig. 8c) by using image processing software.

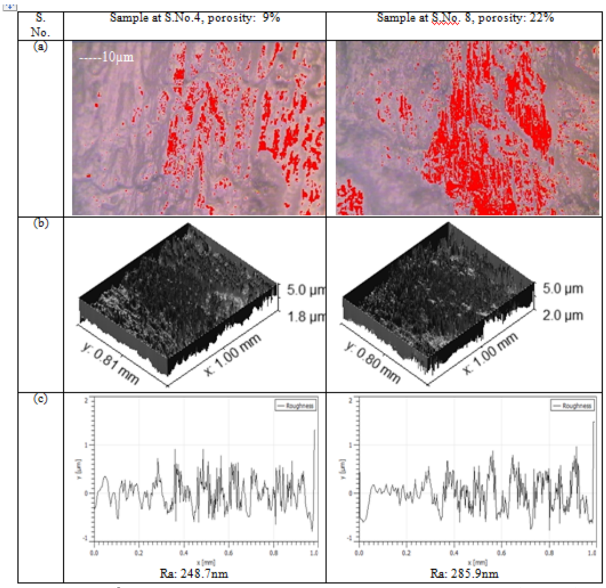

Fig. 8: Surface porosity as per ASTM E2015-04(2014) at ×100 magnification (a), 3D rendered image (b), Ra profile at cut-off length of 0.04mm

As observed from Fig. 8, porosity in sample at S.No. 4 was 9% that is significantly lower from sample at S.No.8,(whose porosity was 22%). This data is also cross verified by 3D rendered image (which shows better distribution of reinforcements in PLA matrix for sample at S.No.4), Ra value and its profile (which is also lower for sample at S.No.4) along with Shore D hardness samples. It should be noted that the hardness of sample at S.No. 4 was best (72) among all samples and hardness of sample at S.No. 8 was observed worst (52) among all samples.

CONCLUSIONS

Following are the conclusions from the present study:

1. The joining of PLA-PEKK-HAp-CS based 3D printed scaffolds is feasible. Although some reduction in peak strength (from 42.29 to 22MPa) was observed (Table 1 and Table 3). But this reduction in peak strength can be justified for small repair/ maintenance of cracked surface of scaffolds. It should be noted that the observed value of peak strength after FSSW is still acceptable in clinical dentistry and for some cases in orthopedic scaffolds. The hardness of joint prepared by FSSW is also acceptable for scaffolds.
2. The best setting of input parameters for peak strength and surface hardness is 1000rpm rotational speed, 2mm consumable pin depth and 20 s stirring time. Further model equations (1 and 2) for peak strength and Shore D hardness has been developed based upon historical data approach.

The present study has been conducted only from optimization view point of mechanical and surface properties with limited input parameters. Further studies may be performed with more controlled input parameters of FSSW such as friction pressure, which may be controlled with table movement in vertical milling setup and corresponding force acting in Z-direction may be calculated through dynamometer. Also for further analysis in-vivo and in-vitro studies need to be conducted in simulated body fluid as per selected application.

ACKNOWLEDGMENT

The authors are thankful to SERB (File No. IMRC/AISTDF/R&D/P-10/2017) for financial support.

REFERENCES

Adam G A, Zimmer D 2015 On design for additive manufacturing: evaluating geometrical limitations. Rapid Prototyping Journal. 21(6): 662-70

Ahn SH, Montero M, Odell D, Roundy S, Wright PK. 2002 Anisotropic material properties of fused deposition modeling ABS. Rapid prototyping Journal. 8(4): 248-57

Baich L, Manogharan G, Marie H. 2015Study of infill print design on production cost-time of 3D printed ABS parts. International Journal of Rapid Manufacturing. 534:308-19

Banjanin B, Vladic G, Pál M, Balos S, Dramicanin M, Rackov M, Knezevic I. 2018 Consistency analysis of mechanical properties of elements produced by FDM additive manufacturing technology. Matéria (Rio de Janeiro). 23(4)

Croccolo D, De Agostinis M, Olmi G. 2013 Experimental characterization and analytical modelling of the mechanical behaviour of fused deposition processed parts made of ABS-M30. Computational Materials Science. 79:506-18

Dizon JR, Espera Jr AH, Chen Q, Advincula RC. 2018 Mechanical characterization of 3D-printed polymers. Additive Manufacturing. 20:44-67

Durgun I, Ertan R. 2014 Experimental investigation of FDM process for improvement of mechanical properties and production cost. Rapid Prototyping Journal.203:228-35

Eslami S, Ramos T, Tavares PJ, Moreira PM. 2015 Effect of friction stir welding parameters with newly developed tool for lap joint of dissimilar polymers. Procedia Engineering.114:199-207

Es-Said OS, Foyos J, Noorani R, Mendelson M, Marloth R, Pregger BA.2000 Effect of layer orientation on mechanical properties of rapid prototyped samples. Materials and Manufacturing Processes. 151:107-22

Fatimatuzahraa AW, Farahaina B, Yusoff WA.2011 The effect of employing different raster orientations on the mechanical properties and microstructure of Fused Deposition Modeling parts. In2011 IEEE Symposium on Business, Engineering and Industrial Applications (ISBEIA), pp 22-27

Jaiganesh V, Maruthu B, Gopinath E. 2014Optimization of process parameters on friction stir welding of high density polypropylene plate. Procedia Engineering. 97:1957-65

Kumar, R., Singh, R., & Ahuja, I. P. S. 2018c. Melt processing for enhancing compatibility of aluminum-reinforced acrylonitrile–butadiene–styrene and polyamide 6 for friction welding applications. Journal of the Brazilian Society of Mechanical Sciences and Engineering, 40(8), 378.

Kumar, R., Singh, R., Ahuja, I. P. S., Penna, R., and Feo, L. 2018a. Weldability of thermoplastic materials for friction stir welding-A state of art review and future applications. Composites Part B: Engineering, 137, 1-15.

Kumar, R., Singh, R., and Ahuja, I. P. S. 2018b. Investigations of mechanical, thermal and morphological properties of FDM fabricated parts for friction welding applications. Measurement, 120, 11-20.

Kumar, R., Singh, R., and Ahuja, I. P. S. 2019. Friction stir welding of ABS-15Al sheets by introducing compatible semi-consumable shoulder-less pin of PA6-50Al. Measurement, 131, 461-472.

Lee BH, Abdullah J, Khan ZA. 2005Optimization of rapid prototyping parameters for production of flexible ABS object. Journal of materials processing technology. 169:154-61

Onwubolu GC, Rayegani F.2014 Characterization and optimization of mechanical properties of ABS parts manufactured by the fused deposition modelling process. International Journal of Manufacturing Engineering.1-13

Ranjan, N., Singh, R., and Ahuja, I. P. S. (2018). Development of PLA-HAp-CS-based biocompatible functional prototype
Ranjan, N., Singh, R., and Ahuja, I. P. S. 2019. Investigations on joining of orthopaedic scaffold with rapid tooling. Proceedings of the Institution of Mechanical Engineers, Part H: Journal of Engineering in Medicine, 0954411919852811.
Rankouhi B, Javadpour S, Delfanian F, Letcher T. 2016Failure analysis and mechanical characterization of 3D printed ABS with respect to layer thickness and orientation. Journal of Failure Analysis and Prevention. 163:467-81
Rankouhi B, Javadpour S, Delfanian F, McTaggart R, Letcher T.2018 Experimental Investigation of Mechanical Performance and Printability of Gamma-Irradiated Additively Manufactured ABS. Journal of Materials Engineering and Performance. 277:3643-54
Rodríguez J F, Thomas J P, Renaud J E 2001 Mechanical behavior of acrylonitrile butadiene styrene (ABS) fused deposition materials. Experimental investigation. Rapid Prototyping Journal. 173:148-58
Senatov, F. S., Niaza, K. V., Zadorozhnyy, M. Y., Maksimkin, A. V., Kaloshkin, S. D., & Estrin, Y. Z. (2016). Mechanical properties and shape memory effect of 3D-printed PLA-based porous scaffolds. Journal of the mechanical behavior of biomedical materials, 57: 139-148
Serra, T., Planell, J. A., & Navarro, M. (2013). High-resolution PLA-based composite scaffolds via 3-D printing technology. Acta biomaterialia, 9(3): 5521-5530
Singh, J., Singh, R., Kumar, R., Rahman, M. M., & Ramakrishna, S. 2019a. PLA-PEKK-HAp-CS composite scaffold joining with friction stir spot welding. Journal of Thermoplastic Composite Materials, 0892705719850609.
Singh, R., Kumar, R., Feo, L., and Fraternali, F. 2016 Friction welding of dissimilar plastic/polymer materials with metal powder reinforcement for engineering applications. Composites Part B: Engineering, 101, 77-86.
Singh, R., Singh, G., Singh, J., and Kumar, R. 2019b. Investigations for tensile, compressive and morphological properties of 3D printed functional prototypes of PLA-PEKK-HAp-CS. Journal of Thermoplastic Composite Materials, 0892705719870595.
Sood AK, Ohdar RK, Mahapatra SS.2010 Parametric appraisal of mechanical property of fused deposition modelling processed parts. Materials & Design.311:287-95
Tian, X., Liu, T., Yang, C., Wang, Q., & Li, D. (2016). Interface and performance of 3D printed continuous carbon fiber reinforced PLA composites. Composites Part A: Applied Science and Manufacturing, 88: 198-205
Vijendra B, Sharma A.2015 Induction heated tool assisted friction-stir welding (i-FSW): a novel hybrid process for joining of thermoplastics. Journal of Manufacturing Processes.20:234-44
Węglowska A, Pietras A.2012 Influence of the welding parameters on the structure and mechanical properties of vibration welded joints of dissimilar grades of nylons. Archives of Civil and Mechanical Engineering.122:198-204